

Semianalytical thermal analysis of rectangle Nd:GGG in heat capacity laser

L.L. Zhang · P. Shi · L. Li

Received: 9 December 2009 / Revised version: 27 February 2010 / Published online: 17 April 2010
© Springer-Verlag 2010

Abstract Based on the theory of anisotropy semianalytical thermal analysis, the temperature field of rectangle Nd:GGG heat capacity laser crystal is investigated. Through an analysis of the working characteristics of the heat capacity laser crystal, a thermal model of heat capacity laser crystal is established. Using a new method for the anisotropic medium heat conduction equation, a temperature field expression of rectangle Nd:GGG heat capacity laser crystal for pumping stage and cooling stage is obtained, respectively. These results show that when using the output power of 300 W LD end-pumped rectangle Nd:GGG crystal for 10 seconds, the maximum temperature rise in the center of the pump face is 180.18°C, and after stopping pumping for 100 seconds, the maximum temperature rise drops to 0.74%. These results from this work provide a theoretical basis for the optimized design of a LD end-pumped heat capacity laser.

1 Introduction

Research on solid state heat capacity laser (SSHCL) has been a hot subject during past few years [1, 2]. SSHCL is a new effective way to improve the thermal effects in which pumping and cooling phase are sequential. It greatly reduces the internal temperature gradient, thermal stress, the optical path distortion and has good beam quality. Heat capacity lasers have a wide range of applications such as laser weapons, industry and scientific research [1, 2].

When pump light energy is absorbed by a heat capacity laser, laser radiation is generated and some pump energy will be converted to thermal energy, non-uniform temperature field and thermal effects such as thermal strain, thermal stress, optical path distortion, thermal lens within the crystal will be generated [1–3]. With the development of laser technology and applications, heat capacity laser output power has reached a few kilowatts, tens of thousands of watts [3]. Thermal effects are not ignored for the design of new novel lasers. The key fundamental work of analysis of thermal effects is to calculate accurately a non-uniform temperature field within laser crystal. A semianalytical thermal analysis method is an effective way to obtain a non-uniform temperature field within laser crystal.

The temperature field is independent on time for all solid state lasers (DPSSL) in steady state. Much thermal effect research of DPSSL has been made [4, 5]. However, the temperature field of solid heat capacity laser is dependent on time. In this paper, using anisotropy semianalytical thermal analysis, the temperature field expression of rectangle Nd:GGG heat capacity laser crystal with Gaussian distribution [6] is investigated. The method can be applied to thermal analysis of other similar laser crystal and provides some references for design of heat capacity laser.

2 Thermal analysis within the Nd:GGG crystal for pumping stage

2.1 Thermal model analysis of rectangle Nd:GGG laser crystal

A thermal analysis physics model of LD end-pumped rectangle Nd:GGG heat capacity laser with a Gaussian distribution is shown in Fig. 1. The size of Nd:GGG rectangle crystal is $a \times b \times c$.

L.L. Zhang (✉) · P. Shi · L. Li
Department of Physics, School of Science, Xi'an University
of Architecture & Technology, 710055 Xi'an, China
e-mail: shengzhxhll@gmail.com

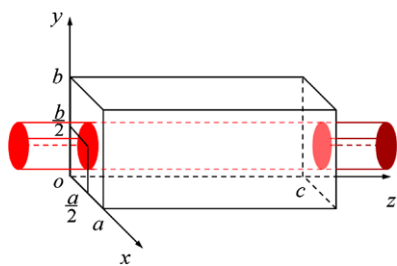


Fig. 1 Thermal model of rectangle Nd:GGG crystals

An LD pump passes through an optical lens system or a coupler composed of a self-focusing lens, and then it will get to the surface of the laser crystal, of which the spatial distribution of the pump light intensity can be approximately expressed by a Gaussian function. If the pump light centered along the crystal axis is injected to the plane $z = 0$ in the z direction, the description of pump light (incident light) distribution on the plane $z = 0$ is given by [5]

$$I(x, y, 0) = I_0 e^{-2 \frac{(x-\frac{a}{2})^2 + (y-\frac{b}{2})^2}{w^2}} \tag{1}$$

Here, I is the pumping light intensity, I_0 is the pump intensity in the center of the pump light, and w is the Gaussian radius of pump beam. If the absorption coefficient of the laser crystal about pump light is β , and the pump light propagates along the z axis, then the light intensity will be weakened due to absorption. According to the absorption law, the light intensity on the plane $z = z$ within the crystal is given by $I(x, y, z) = I(x, y, 0) \cdot e^{-\beta z}$. Thus the thermal power density on the plane $z = z$ is given by [4, 5]:

$$q_V(x, y, z) = I_0 \eta \beta e^{-2 \frac{(x-\frac{a}{2})^2 + (y-\frac{b}{2})^2}{w^2}} \cdot e^{-\beta z} \tag{2}$$

in which η is a thermal conversion fraction.

2.2 Semianalytical calculation expression of temperature field within rectangle Nd:GGG laser crystal

As there is a heat source within the heat capacity laser crystal for pumping stage ($0 < t < t_1$), the distribution of the temperature field $u(x, y, z, t)$ follows the Poisson equation,

$$\rho C \frac{\partial u}{\partial t} = \lambda_x \frac{\partial^2 u}{\partial x^2} + \lambda_y \frac{\partial^2 u}{\partial y^2} + \lambda_z \frac{\partial^2 u}{\partial z^2} + q_V(x, y, z) \tag{3}$$

where $\lambda_x, \lambda_y, \lambda_z$ is the coefficient of heat conductivity along the x, y, z direction, respectively, ρ is the mass density of the laser crystal, C is the specific heat capacity. We suppose the crystal coordinates to obey ($0 < x < a, 0 < y < b, 0 < z < c$).

In order to maintain a good thermal contact between laser rod and thermal sink, firstly silicone grease of ther-

mal conduction is coated on side faces of the laser rod, then the whole is wrapped with indium and placed in the folder block of copper thermal sink. In addition, the crystal is edge-cooled to a relatively constant temperature, which can be assumed to be u_w and in the mathematical treatment of a thermal model it can be set at zero, so long as the cooling temperature u_w is added to the ultimately calculated temperature field. The two end faces of the rectangle Nd:GGG crystal can be adiabatic, for the coefficient of heat transfer between the two end faces of crystal and air is very small. Therefore boundary conditions of the thermal model can be expressed by [1]

$$\begin{aligned} u(0, y, z, t) &= 0, & u(a, y, z, t) &= 0, \\ u(x, 0, z, t) &= 0, & u(x, b, z, t) &= 0, \\ \frac{\partial u(x, y, z, t)}{\partial z} \Big|_{z=0} &= 0, & \frac{\partial u(x, y, z, t)}{\partial z} \Big|_{z=c} &= 0. \end{aligned}$$

At the beginning of pumping, the initial temperature of the laser crystal is zero (relatively), then the initial condition is $u(x, y, z, 0) = 0$.

A method to solve heat conduction equation with given boundary conditions is as follows. (1) The form of the family of the eigenfunction in the heat conduction equation can be determined according to the boundary conditions, and the family of eigenfunctions can constitute the solution of heat conduction, in which there are some constants to be determined. (2) The general solution is then substituted into the heat conduction equation to obtain the expression of the undetermined constants. The expression of the temperature field satisfies both the heat conduction equation and its boundary conditions, and the solution of the heat conduction equation is unique; therefore the expression of the temperature field should be the unique solution of the heat conduction equation [4, 5].

According to the boundary condition, the family of eigenfunctions of x, y and z is $\sin \frac{n\pi}{a}x, \sin \frac{m\pi}{b}y, \cos \frac{l\pi}{c}z$, respectively [7], where n, m, l is integer. So the solution of the heat conduction equation can be assumed to be

$$u(x, y, z, t) = \sum_{n=0}^{\infty} \sum_{m=0}^{\infty} \sum_{l=1}^{\infty} A_{nml}(t) \sin \frac{n\pi}{a}x \sin \frac{m\pi}{b}y \cos \frac{l\pi}{c}z, \tag{4}$$

where $A_{nml}(t)$ is a constant to be determined. The expression of $u(x, y, z, t)$ can be substituted into the Poisson equation to confirm its detailed form:

$$\begin{aligned} \rho C \sum_{n=0}^{\infty} \sum_{m=0}^{\infty} \sum_{l=1}^{\infty} \frac{dA_{nml}(t)}{dt} \sin \frac{n\pi}{a}x \sin \frac{m\pi}{b}y \cos \frac{l\pi}{c}z \\ = - \sum_{n=0}^{\infty} \sum_{m=0}^{\infty} \sum_{l=1}^{\infty} A_{nml}(t) \left[\lambda_x \left(\frac{n\pi}{a} \right)^2 + \lambda_y \left(\frac{m\pi}{b} \right)^2 \right] \end{aligned}$$

$$\begin{aligned}
 & + \lambda_z \left(\frac{l\pi}{c} \right)^2 \left] \sin \frac{n\pi}{a} x \sin \frac{m\pi}{b} y \cos \frac{l\pi}{c} z \right. \\
 & \left. + q_V(x, y, z). \right. \tag{5}
 \end{aligned}$$

Suppose the constant C_1 has the following form,

$$C_1 = \frac{1}{\rho C} \left[\lambda_x \left(\frac{n\pi}{a} \right)^2 + \lambda_y \left(\frac{m\pi}{b} \right)^2 + \lambda_z \left(\frac{l\pi}{c} \right)^2 \right].$$

According to the orthogonality and normalization of the x eigenfunction, we have $\int_0^a \sin \frac{n\pi}{a} x \sin \frac{k\pi}{a} x dx = \frac{a}{2} \delta_{nk}$. Both sides of (5) are multiplied with $\sin \frac{k\pi}{a} x$ and integrating over x from 0 to a yields:

$$\begin{aligned}
 & \sum_{m=0}^{\infty} \sum_{l=1}^{\infty} \left[\frac{dA_{nml}(t)}{dt} + C_1 A_{nml}(t) \right] \sin \frac{m\pi}{b} y \cos \frac{l\pi}{c} z \\
 & = \frac{2}{a\rho C} \int_0^a q_V(x, y, z) \sin \frac{n\pi}{a} x dx. \tag{6}
 \end{aligned}$$

According to the above analysis of x variable, variables y and z have similar processes, respectively,

$$\begin{aligned}
 & \frac{dA_{nml}(t)}{dt} + C_1 A_{nml}(t) \\
 & = \frac{8}{abc\rho C} \int_0^c \int_0^b \int_0^a q_V(x, y, z) \sin \frac{n\pi}{a} x \sin \frac{m\pi}{b} y \\
 & \quad \times \cos \frac{l\pi}{c} z dx dy dz. \tag{7}
 \end{aligned}$$

If the constant $C_2 = \frac{8}{abc\rho C} \int_0^c \int_0^b \int_0^a q_V(x, y, z) \sin \frac{n\pi}{a} x \sin \frac{m\pi}{b} y \cos \frac{l\pi}{c} z dx dy dz$, (7) is simplified to the following form:

$$\frac{dA_{nml}(t)}{dt} = -C_1 A_{nml}(t) + C_2. \tag{8}$$

Equation (8) is an ordinary differential equation, the solution is of the following form $A_{nml}(t) = \frac{C_2}{C_1} + C_3 e^{-C_1 t}$, where C_3 is an undetermined constant. According to the initial conditions, $u(x, y, z, 0) = 0$ when $t = 0$, so the following constant can be obtained: $A_{nml}(0) = 0$. Substituting the constant into (8) yields $C_3 = -\frac{C_2}{C_1}$. Further substituting the constants C_1, C_2, C_3 and (2) into (8) may yield the following form:

$$\begin{aligned}
 A_{nml}(t) & = \frac{8I_0\eta\beta}{abc[\lambda_x(\frac{n\pi}{a})^2 + \lambda_y(\frac{m\pi}{b})^2 + \lambda_z(\frac{l\pi}{c})^2]} \\
 & \quad \times \left(1 - e^{-\frac{1}{\rho C}[\lambda_x(\frac{n\pi}{a})^2 + \lambda_y(\frac{m\pi}{b})^2 + \lambda_z(\frac{l\pi}{c})^2]t} \right) \\
 & \quad \times \int_0^c \int_0^b \int_0^a e^{-2\frac{(x-\frac{a}{2})^2 + (y-\frac{b}{2})^2}{w^2}} e^{-\beta z} \sin \frac{n\pi}{a} x \\
 & \quad \times \sin \frac{m\pi}{b} y \cos \frac{l\pi}{c} z dx dy dz. \tag{9}
 \end{aligned}$$

Therefore (4) is the solution to the heat conduction equation in heat capacity laser crystals for pumping stage and coefficients in (4) can be determined by (9).

2.3 Temperature field analysis in rectangle Nd:GGG laser crystal for pumping stage

The pump power of the diode laser is 300 W. The Gaussian radius of the pump light is 9.00 mm and the size of the rectangle crystal is 40 mm × 40 mm × 18 mm. For a rectangle Nd:GGG crystal doped with 0.6% Nd³⁺, the absorption coefficient of the crystal about pump light (808 nm) is 1.8 cm⁻¹, the coefficient of heat conductivity is 9 W m⁻¹ K⁻¹, the mass density is 7100 kg m⁻³ and the specific heat capacity is 410 J/(kg K) and the thermal conversion fraction η is 0.3 [8]. The distribution of the calculated temperature field on the end face $y = b/2$ within the crystal pumped for 10 seconds is shown in Fig. 2, and the isotherm distribution is shown in Fig. 3. The maximum temperature rise in the rectangle Nd:GGG crystal is 180.18°C located at $x = a/2, y = b/2, z = 0$ in the center of the pump face. The maximum temperature rise located at $x = a/2, y = b/2, z = 0$ as a function of pump time is shown in Fig. 4.

In Fig. 4 it can be seen that the maximum temperature rise increases rapidly with pump time at the beginning, then it increases slowly and reached a maximum value pumped about 120 seconds, which is the saturation temperature (the cooling system has been working since starting pump, it can form a saturation temperature). The percentage of the maximum temperature rise to saturation temperature for different pump times of 1 s, 2 s, 3 s, 4 s, 5 s, 15 s, 20 s, 30 s is 12.9%, 21.9%, 28.8%, 34.5%, 39.2%, 64.9%, 71.8%, 81.2%, respectively. For the design of the heat capacity laser, according to the maximum allowable temperature rise, the maximum pump time of heat capacity laser can be calculated.

To change the function form of thermal power density within crystal, one may study another thermal analysis, such as double-end-pumped (according to the above derivation, when the double-end-pumped function form of thermal power density substitutes for the single-end-pumped function form of thermal power density, it can be concluded to

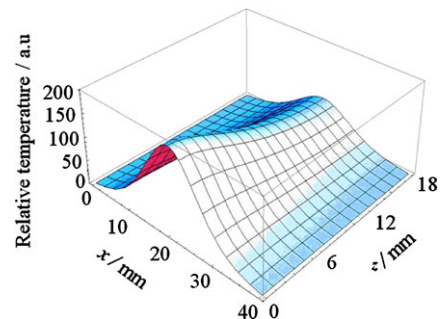


Fig. 2 Temperature field distribution diagram of a rectangle Nd:GGG crystal on the end face $y = b/2$ pumped for 10 seconds

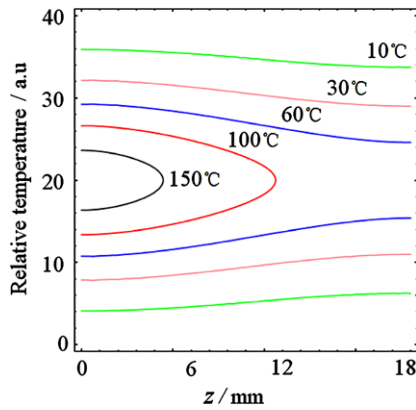


Fig. 3 Isotherm diagram of a rectangle Nd:GGG crystal pumped for 10 seconds

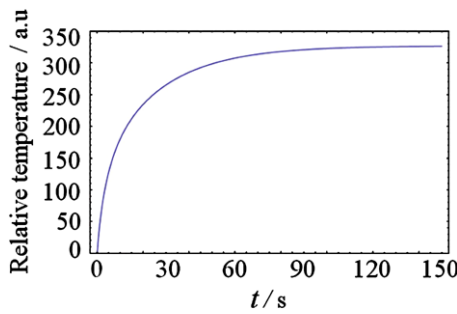


Fig. 4 The maximum temperature rise located at $x = a/2, y = b/2, z = 0$ as a function of pump time

the double-end-pumped calculation expression of the temperature field).

Changing a variable of the heat conduction equation expression, the influence of the variable on the temperature field can be studied. A quantity such as the influence of size with Gaussian ring of light on the temperature field in rectangle crystals can be calculated and analyzed.

In [8] the author studied the thermal analysis of end-pumped Nd:GGG heat capacity laser. Using our calculation method in this paper, we simulated the heat capacity laser which they have studied. The result shows that the temperature field distribution within crystal and the maximum temperature rise is consistent with that in [8]. So it is proved that the conclusion of this paper is correct.

3 Thermal analysis within the crystal for cooling stage

3.1 Calculation expression of temperature field within crystal for cooling stage

When the heat capacity laser stops pumping and is going to the cooling stage ($t_1 < t < t_2$), as there is no heat source

within the heat capacity laser crystal for cooling stage, the distribution of the temperature field $T(r, z, t)$ follows the heat transfer equation,

$$\rho C \frac{\partial T}{\partial t} = \lambda_x \frac{\partial^2 T}{\partial x^2} + \lambda_y \frac{\partial^2 T}{\partial y^2} + \lambda_z \frac{\partial^2 T}{\partial z^2}. \tag{10}$$

The boundary conditions are similar with the above mentioned boundary conditions

$$\begin{aligned} T(0, y, z, t) &= 0, & T(a, y, z, t) &= 0, \\ T(x, 0, z, t) &= 0, & T(x, b, z, t) &= 0, \\ \frac{\partial T(x, y, z, t)}{\partial z} \Big|_{z=0} &= 0, & \frac{\partial T(x, y, z, t)}{\partial z} \Big|_{z=c} &= 0. \end{aligned}$$

The Moment of pumping cessation is the moment of cooling stage. So the initial conditions of cooling stage is $T(x, y, z, t_1) = u(x, y, z, t_1)$.

For the variables of heat transfer equation are separated, the solution to heat transfer equation is supposed to be the following form: $T(x, y, z, t) = \tau(t)X(x)Y(y)Z(z)$, then it can be substituted into the heat transfer equation, yields

$$\begin{aligned} \rho C \frac{1}{\tau(t)} \frac{d\tau(t)}{dt} &= \lambda_x \frac{1}{X(x)} \frac{\partial^2 X(x)}{\partial x^2} + \lambda_y \frac{1}{Y(y)} \frac{\partial^2 Y(y)}{\partial y^2} \\ &+ \lambda_z \frac{1}{Z(z)} \frac{\partial^2 Z(z)}{\partial z^2}. \end{aligned} \tag{11}$$

If both sides of (11) are equal to the constant C_4 , there are three different variables among three terms, respectively, on the right side of (14). On further separation of the variables, the right side of (14) is satisfied by the following condition:

$$\begin{aligned} \lambda_x \frac{1}{X(x)} \frac{\partial^2 X(x)}{\partial x^2} &= -C_x; & \lambda_y \frac{1}{Y(y)} \frac{\partial^2 Y(y)}{\partial y^2} &= -C_y; \\ \lambda_z \frac{1}{Z(z)} \frac{\partial^2 Z(z)}{\partial z^2} &= -C_z; & C_x + C_y + C_z &= -C_4 \end{aligned} \tag{12}$$

where C_x, C_y, C_z, C_4 are constants, respectively. The term contained x is simplified into the form $\frac{\partial^2 X(x)}{\partial x^2} + \frac{C_x}{\lambda_x} X(x) = 0$, so the general solution contained is $X(x) = A \sin(\sqrt{\frac{C_x}{\lambda_x}} x) + B \cos(\sqrt{\frac{C_x}{\lambda_x}} x)$.

According to the boundary condition of x direction $X(0) = 0, X(a) = 0$, the constant B and C_x is determined $B = 0, C_x = \lambda_x (\frac{n\pi}{a})^2$. So the term $X(x)$ is obtained with the following form

$$X(x) = A_1 \sin \frac{n\pi}{a} x. \tag{13}$$

Similarly, the constant C_y and C_z are obtained $C_y = \lambda_y (\frac{m\pi}{b})^2, C_z = \lambda_z (\frac{l\pi}{c})^2$, and the terms $Y(y)$ and $Z(z)$ are of the following form, respectively,

$$Y(y) = A_2 \sin \frac{m\pi}{b} y, \tag{14}$$

$$Z(z) = A_3 \cos \frac{l\pi}{c} z \tag{15}$$

where A_1, A_2, A_3 is constant, respectively. So the following form is obtained:

$$X(x)Y(y)Z(z) = \sum_{n=0}^{\infty} \sum_{m=0}^{\infty} \sum_{l=1}^{\infty} A_1 A_2 A_3 \sin \frac{n\pi}{a} x \sin \frac{m\pi}{b} y \cos \frac{l\pi}{c} z. \tag{16}$$

The constant C_4 is of the form:

$$C_4 = -C_x - C_y - C_z = -\left[\lambda_x \left(\frac{n\pi}{a} \right)^2 + \lambda_y \left(\frac{m\pi}{b} \right)^2 + \lambda_z \left(\frac{l\pi}{c} \right)^2 \right]. \tag{17}$$

The term contained t is simplified into the form: $\frac{d\tau(t)}{\tau(t)} = C_4 \frac{\lambda}{\rho c} dt$. It is an ordinary differential equation and the solution is $\tau(t) = C_5 e^{C_4 \frac{\lambda}{\rho c} (t-t_1)}$, where C_5 is a constant. Therefore the solution to temperature field is obtained in the following form:

$$T(x, y, z, t) = \sum_{n=0}^{\infty} \sum_{m=0}^{\infty} \sum_{l=1}^{\infty} B_{nml} e^{-\frac{1}{\rho c} [\lambda_x (\frac{n\pi}{a})^2 + \lambda_y (\frac{m\pi}{b})^2 + \lambda_z (\frac{l\pi}{c})^2] (t-t_1)} \times \sin \frac{n\pi}{a} x \sin \frac{m\pi}{b} y \cos \frac{l\pi}{c} z \tag{18}$$

where $B_{nml} = C_5 A_1 A_2 A_3$ is a constant to be determined. According to the initial conditions, when $t = t_1$, the detailed form of the solution to the heat transfer equation is

$$T(x, y, z, t_1) = \sum_{n=0}^{\infty} \sum_{m=0}^{\infty} \sum_{l=1}^{\infty} B_{nml} \sin \frac{n\pi}{a} x \sin \frac{m\pi}{b} y \cos \frac{l\pi}{c} z = u(x, y, z, t_1) = \sum_{n=0}^{\infty} \sum_{m=0}^{\infty} \sum_{l=1}^{\infty} A_{nml}(t_1) \sin \frac{n\pi}{a} x \sin \frac{m\pi}{b} y \cos \frac{l\pi}{c} z. \tag{19}$$

So the coefficient B_{nml} can be determined by (20).

$$B_{nml} = A_{nml}(t_1) = \frac{8I_0 \beta^2 \eta c (1 - e^{-\beta c} \cos l\pi)}{ab(\beta^2 c^2 + l^2 \pi^2) [\lambda_x (\frac{n\pi}{a})^2 + \lambda_y (\frac{m\pi}{b})^2 + \lambda_z (\frac{l\pi}{c})^2]}$$

$$\times \left(1 - e^{-\frac{1}{\rho c} [\lambda_x (\frac{n\pi}{a})^2 + \lambda_y (\frac{m\pi}{b})^2 + \lambda_z (\frac{l\pi}{c})^2] t_1} \right) \times \int_0^b \int_0^a e^{-2 \frac{(x-a/2)^2 + (y-b/2)^2}{w^2}} \sin \frac{n\pi}{a} x \sin \frac{m\pi}{b} y dx dy. \tag{20}$$

Therefore (18) is the solution to the heat transfer equation in rectangle heat capacity crystals for cooling stage ($t_1 < t < t_2$) and the coefficient of B_{nml} can be determined by (20).

3.2 Temperature field analysis in rectangle Nd:GGG laser crystal for cooling stage

According to the conditions and parameters in Fig. 2, when the rectangle Nd:GGG laser is pumped for 10 seconds and stopped pumping into the cooling stage, the temperature field in rectangle Nd:GGG crystals is calculated and analyzed. The maximum temperature rise located at $x = a/2, y = b/2, z = 0$ with cooling time is shown in Fig. 5. After stopping pumping into cooling for 100 seconds, the maximum temperature rise drops to 0.74% that is 1.3°C. The distribution of the calculated temperature field within the crystal cooled for 100 seconds is shown in Fig. 6.

Defining the cooling time as the temperature rise at which we have 0.74% of the maximum temperature rise, it can be seen that after having cooled for 100 seconds the crystal, the temperature within crystal approaches the cooling

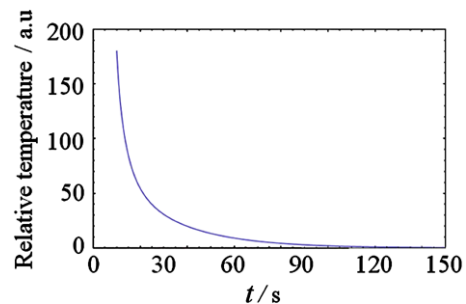


Fig. 5 The attention of the maximum temperature rise located at $x = a/2, y = b/2, z = 0$ with cooling time

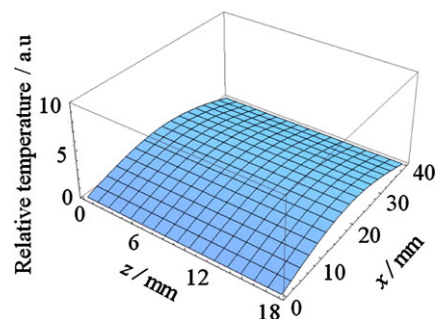


Fig. 6 Temperature field distribution diagram of a rectangle Nd:GGG cooled for 100 seconds

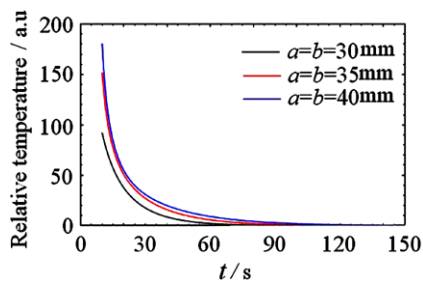


Fig. 7 The maximum temperature rise as a function of cooling time under different length

medium temperature, and there is no axial temperature gradient. Then the next pump cycle can be started.

According to (18), the influence of different parameters on cooling time can be studied, such as the influence of crystal length on cooling time, which can be calculated and analyzed. When the side length of the rectangle crystal a and b is equal to 30 mm, 35 mm and 40 mm, respectively, and other conditions are unchanged, the maximum temperature rise located at $x = a/2$, $y = b/2$, $z = 0$ with cooling time is shown in Fig. 7. From Fig. 7, it can be seen that the bigger the side length, the longer the cooling time required for edge cooling. When the side length $a = b = 40$ mm and $a = b = 30$ mm, the required cooling times were 100 s and 60 s, respectively.

4 Conclusion

In this paper, based on anisotropy semianalytical thermal analysis method, an expression of the temperature field of

rectangle Nd:GGG heat capacity laser with Gaussian distribution for LD end-pumped stage is obtained and it provides a theoretical basis for calculating and choosing pumping time of heat capacity laser. The formula for calculating the temperature field within rectangle crystal for cooling stage is achieved and analyzed quantitatively. Similarly, it provides a theoretical basis for choosing cooling time of heat capacity laser. The semianalytical method in this paper can be used to calculate the temperature field in other heat capacity laser crystals. Based on the method proposed in this paper and using the conclusion, thermal distortion field, thermal focal length and so on can be further investigated. The results from this work offer a theoretical base for the optimization design of heat capacity laser.

Acknowledgements This work is supported by the Education Special Projects of Shaanxi Province Office under Grant 09JK536 and the Industrial Research Project Funding of Technology Department of Shaanxi Province under Grant 2008K05-15.

References

1. X.Q. Li, Z.G. Dou, Q. Li, M. Wen, C.Y. Cui, J. Acad. Equip. Command Technol. **19**, 95 (2008)
2. B.S. Wang, H.H. Jiang, Q.L. Zhang, D.L. Sun, S.T. Yin, L.F. Li, S.H. Shao, Chin. J. Quantum Electron. **24**, 688 (2007)
3. H. Hu, Z. Cai, J.F. Jiang, B. Tu, Z.P. Pei, T.J. Zhou, Y. Cheng, Chin. J. Lasers **34**, 1507 (2007)
4. P. Shi, W. Chen, L. Li, A. Gan, Appl. Opt. **46**, 4046 (2007)
5. P. Shi, W. Chen, L. Li, A. Gan, Appl. Opt. **46**, 6655 (2007)
6. J.M. Li, Laser Optoelectron. Prog. **45**, 16 (2008)
7. M. Sabaeian, H. Nadgaran, C. Mousave, Appl. Opt. **47**, 2317 (2008)
8. J.K. Yang, D.X. Cao, W.G. Zhen, S.B. He, X.D. Yuan, H.W. Yu, W. Han, Laser Technol. **31**, 196 (2007)